



HHS Public Access

Author manuscript

Biochemistry. Author manuscript; available in PMC 2017 November 01.

Published in final edited form as:

Biochemistry. 2017 June 27; 56(25): 3178–3183. doi:10.1021/acs.biochem.7b00271.

Expanding the Scope of Electrophiles Capable of Targeting K-Ras Oncogenes

Lynn M. McGregor^{†,ID}, Meredith L. Jenkins[‡], Caitlin Kerwin[†], John E. Burke^{‡,ID}, and Kevan M. Shokat^{*,†,ID}


[†]Howard Hughes Medical Institute and Department of Cellular and Molecular Pharmacology, University of California, San Francisco, San Francisco, California 94158, United States

[‡]Department of Biochemistry and Microbiology, University of Victoria, Victoria, BC V8W 2Y2, Canada

Abstract

There is growing interest in reversible and irreversible covalent inhibitors that target noncatalytic amino acids in target proteins. With a goal of targeting oncogenic K-Ras variants (e.g., G12D) by expanding the types of amino acids that can be targeted by covalent inhibitors, we survey a set of electrophiles for their ability to label carboxylates. We functionalized an optimized ligand for the K-Ras switch II pocket with a set of electrophiles previously reported to react with carboxylates and characterized the ability of these compounds to react with model nucleophiles and oncogenic K-Ras proteins. Here, we report that aziridines and stabilized diazo groups preferentially react with free carboxylates over thiols. Although we did not identify a warhead that potently labels K-Ras G12D, we were able to study the interactions of many electrophiles with K-Ras, as most of the electrophiles rapidly label K-Ras G12C. We characterized the resulting complexes by crystallography, hydrogen/deuterium exchange, and differential scanning fluorimetry. Our results both demonstrate the ability of a noncatalytic cysteine to react with a diverse set of electrophiles and emphasize the importance of proper spatial arrangements between a covalent inhibitor and its intended nucleophile. We hope that these results can expand the range of electrophiles and nucleophiles of use in covalent protein modulation.

*Corresponding Author. kevan.shokat@ucsf.edu.

ORCID 

Lynn M. McGregor: 0000-0003-4310-2384

John E. Burke: 0000-0001-7904-9859

Kevan M. Shokat: 0000-0002-6900-8380

ASSOCIATED CONTENT

Supporting Information

The Supporting Information is available free of charge on the [ACS Publications website](https://pubs.acs.org) at DOI: 10.1021/acs.biochem.7b00271.

Supporting figures, tables, and methods ([PDF](#))

Accession Codes

The co-crystal structures of K-Ras G12C bound to **1** and **3** have been deposited as Protein Data Bank entries 5V6S and 5V6V, respectively.

The authors declare the following competing financial interest(s): K.M.S. is an inventor on UCSF patents related to K-Ras (G12C) inhibitors licensed to Wellspring Biosciences. K.M.S. is a stockholder and consultant to Wellspring Biosciences.

Ras is a small GTPase that switches between an active, GTP-bound state and an inactive, GDP-bound state.¹ Oncogenic mutations that decrease the level of GTP hydrolysis contribute to >30% of cancers.² Ras has been the subject of many drug discovery efforts, leading to the identification of inhibitors that block the membrane localization of Ras or its ability to bind effectors. Lacking deep hydrophobic pockets, direct inhibitors of Ras engage one or more shallow pockets^{3–7} or bind covalently to an acquired cysteine 12.^{8,9} The requirement for Cys12 limits the application of these compounds in cancers with other Ras mutations. We wondered whether an electrophilic Ras ligand could covalently label K-Ras G12D, a mutation found in >30% of Ras mutant cancers.²

Recently, there has been a dramatic increase in the level of interest in irreversible and reversible covalent inhibitors that target catalytic or noncatalytic amino acids.^{10–17} Because of our interest in Ras mutant cancers and with a goal of expanding the range of amino acids targeted by covalent inhibitors, we investigated the ability of several functional groups to react with carboxylates. A strategy for proximity-dependent labeling of aspartate or glutamate could find broad use in covalent probes.¹⁸ We wondered if the interaction between an optimized Ras ligand and K-Ras could promote a reaction between G12D and a functional group known to label catalytic carboxylates, such as an epoxide, aziridine, or chloroacetamide.^{17,19–21} We also considered functional groups that have been reported to label noncatalytic aspartate and glutamate residues, such as chloroethylureas,²² stabilized diazo groups,^{23,24} trichloroacetimidates,²⁵ and acyl imidazoles.²⁶ Here, we report the ability of these electrophiles to react with model nucleophiles and to form covalent complexes with K-Ras G12C. Structural characterization of two of these complexes reveals that even minor changes in the electrophile can dramatically alter the compound's binding mode.

RESULTS AND DISCUSSION

We first considered three reported K-Ras G12C switch II pocket scaffolds and compared the rate at which each acrylamide could label K-Ras G12C (Figure S1A).^{8,27,28} The most potent scaffold was synthesized as a mixture of atropisomers, with the indazole up (*R*) or down (*S*), compared to the quinazoline. We elaborated this scaffold with several electrophiles (Figure 1A) and assessed the reactivity of compounds **1–10** toward a model thiol and model carboxylates. Although some of these warheads could react promiscuously, we did not want to exclude any potentially promising electrophiles. By liquid chromatography and mass spectrometry (LC–MS), we found that compounds **1**, **2**, **6**, and **10** readily form adducts with β -mercaptoethanol (BME) in phosphate-buffered saline (Figure 1B). In contrast, compounds **3**, **4**, **7**, and **8** form covalent adducts with *N*-Boc-aspartate and sodium benzoate in a 1:1 acetonitrile/0.1 M MES (pH 6) solution (Figure 1B). Encouragingly, we identified two functional groups with the desired property of preferential reactivity toward carboxylates over a thiol.

We next asked whether these molecules could covalently label K-Ras, using K-Ras G12C 1–169 as a positive control and wild-type (WT) K-Ras 1–169 as a negative control. Each compound (100 μ M) was incubated with Ras (4 μ M) for 24 h at room temperature and pH 7.5. By intact protein LC–MS, we found that most of the compounds could efficiently label K-Ras G12C and that none of the compounds exhibited strong nonspecific labeling of WT

K-Ras (Figure 1C). For compound **8**, we found that 2.6% of the protein corresponded to a mass consistent with double labeling. To study reactivity with Asp12, we made use of a CysLight (CL) variant of K-Ras G12D (1–169; C51S/C80L/C118S), which is intended to eliminate potential sources of nonspecific labeling and increase the level of confidence that any labeling differences observed between variants are caused by the identity of amino acid 12. Covalent adducts between compounds **1–10** and K-Ras G12D CL were not observed. The reactivity of **3**, **4**, **7**, and **8** is expected to increase with a decrease in pH,²³ and we wondered whether a low pH could induce a reaction with G12D. Each compound was incubated with G12C, G12D, G12S, or WT K-Ras CL in buffers with pH values from 7.5 to 5.5. At pH 5.5, we observed a modest increase in reactivity between **3** and the WT, G12S, and G12D proteins (1.0, 2.7, and 4.3% labeled, respectively) (Figure 1D and Figure S1B). We cannot entirely rule out the possibility that G12D covalent adducts are hydrolyzed in solution or during mass spectrometry. Differential scanning fluorimetry (DSF)²⁹ performed on K-Ras G12D CL after treatment with **3**, **4**, **7**, or **8** at pH 5.5 did not show evidence of protein–small molecule interactions. Together, these results suggest that although the reactivity of compounds **3**, **4**, **7**, and **8** is appropriate for carboxylate residues, these compounds cannot efficiently label K-Ras G12D, perhaps because of a poor spatial arrangement between the electrophiles and Asp12.

Structural differences in the electrophiles that covalently label K-Ras G12C are expected to alter their intrinsic reactivity and their pre- and postreaction binding conformations. We analyzed each complex by DSF and found that **1** strongly stabilized K-Ras G12C CL ($T_M = 77.7$ °C) when compared to the unlabeled form of K-Ras G12C CL ($T_M = 55.3$ °C) (Figure 1E and Figure S6A). Interestingly, we found that **4** stabilized K-Ras strongly ($T_M = 74.0$ °C) while **3** only moderately stabilized Ras ($T_M = 61.1$ °C). A racemic epoxide (**2**) produced two distinct melting transitions (Figure S1C,D) that we suspect may correspond to separate melting transitions associated with each isomer. To test this hypothesis, we treated K-Ras G12C with **3** or **4**, confirmed complete labeling by LC–MS, removed excess **3** or **4** with a desalting column, and then combined the purified, labeled protein in several ratios. Indeed, the melting transitions of these mixtures strongly resembled the melting transition of K-Ras G12C CL labeled with **2** (Figure S1E,F). Together, these results suggest that there may be significant differences in the way that **1** and **3** engage the SII-P. Further, we wondered if Cys12 attacks **3** at the α - or β -carbon of the aziridine.

To address these questions, we determined the high-resolution co-crystal structures of GDP-bound K-Ras G12C CL in complex with **1** or **3** (Figures 2, S2, and S4). The overall protein conformation of K-Ras G12C with **1** closely matches that of the complex of K-Ras G12C and ARS-853 (Protein Data Bank entry 5F2E) [root-mean-square deviation (RMSD) of 0.31 Å].²⁷ The structure of switch I is similar to that in other structures of GDP-bound Ras. Switch II and helix $\alpha 2$ adopt a structured conformation that is rotated and farther from the nucleotide binding site and core of the protein than in the first SII-P-bound Ras structures.⁸ Switch II surrounds the ligand, with only a few inhibitor atoms exposed to the solvent (Figure 2A). We observe a bond between common rotamers of Cys12 and the β -carbon of the acrylamide. A hydrophobic pocket formed by Val9, Met72, Phe78, Ile100, and Val103 is occupied by the phenyl and methyl portions of the indazole group. The indazole NH makes a

hydrogen bond with Asp69, located on helix $\alpha 2$ (Figure 2B). The quinazoline N1 atom contacts His95 on helix $\alpha 3$. The carbonyl of the acrylamide hydrogen bonds with Lys16 and with one of the water molecules that coordinates Mg^{2+} . The hydrogen bond with Lys16 may serve to position the acrylamide for attack and could increase its electrophilicity.

In the structure with **3**, we were surprised to find that Cys12 reacts with the more hindered α -carbon of **3** rather than the β -carbon (Figure 2C). Comparing the structures with **1** and **3**, we find that the overall protein conformation is very consistent (RMSD of 0.37 Å), but the quinazoline binding poses differ substantially (Figures 2 and S2). In fact, compounds **1** and **3** bind Ras via opposite atropisomers (*R* and *S*, respectively). Although **3** binds to Cys12, Asp69, and the hydrophobic pocket, its quinazoline N1 atom and carbonyl are oriented opposite to those of **1** and hydrogen bond with Arg68 and the solvent, respectively. The different compound binding poses result in a slightly different conformation in switch II and helix $\alpha 2$ (Figure 2C) (residues 61–72, RMSD of 0.66 Å). Although K-Ras G12C is reported to preferentially react with one atropisomer,²⁸ its ability to react with the other atropisomer emphasizes the flexible nature of the switch II pocket.

To verify that the structures we observed crystallographically reflect the solution state, we next analyzed these complexes by hydrogen–deuterium exchange LC–MS (HDX–MS). This technique has been widely applied to the analysis of protein–small molecule binding interactions³⁰ and has been used to characterize the dynamics of Ras in its GDP, GMPNP, and guanosine mimicking inhibitor-bound states.^{9,31} In this approach, protein dynamics are analyzed by measuring the rate of exchange of amide protons with deuterium. The involvement of amide hydrogens in the secondary structure leads to a decreased level of exchange, and as such, this technique is well suited to probing protein conformational changes. Flexible regions of the protein readily incorporate deuterium, while structured regions are protected from deuterium exchange (Figure 2D). Compared to a previously reported HDX study of guanosine mimic-bound Ras,⁹ we observe a large global decrease in the level of deuterium incorporation in the complexes with **1** and **3**. When differences in the HDX profiles of GDP-bound K-Ras and its complexes with **1** and **3** are mapped onto the corresponding crystal structures, it is clear that **1** protects Ras more strongly than **3** does. This observation confirms the DSF result that shows **1** causes a larger increase in Ras melting temperature than **3** does (Figures 1, 2, and S5). The peptides that contact **1** or **3** are highly protected (Figures 2, S2, and S5). Although compounds **1** and **3** bind the switch II pocket, they also cause protection of the guanosine binding loop (residues 114–125) that is also protected by a covalent guanosine mimic.⁹ In the complex with **1**, peptides corresponding to switch I (residues 33–40), switch II and helix $\alpha 2$ (residues 65–72), and helix $\alpha 3$ (residues 84–99) are all protected. In contrast, **3** promotes protection of helix $\alpha 2$, but not switch I or helix $\alpha 3$. The ability of **1** but not **3** to protect helix $\alpha 3$ agrees with the crystallographic observation that **1** but not **3** forms hydrogen bonds with His95.

We next asked whether the difference between **3** and **4** in DSF could be explained by the ability of Cys12 to react with the corresponding *R* or *S* atropisomer. When each aziridine was modeled onto the structures of **1** and **3**, we noticed that only the *S* atropisomer would position Cys12 anti to the C–N bond of **3** while the *R* atropisomer appropriately positions **4**

for attack (Figure S3). These differences highlight potential challenges and/or selectivity benefits associated with the use of chiral electrophiles in covalent inhibitors.

In the co-crystal structures, we also noticed that the electrophilic portion of the compound is relatively flat and rigid, perhaps preventing a conformation appropriate for a reaction with Asp12. To allow greater rotation of the electrophilic warheads, we replaced the piperazine moiety with 4-aminopiperidine or 3-aminopyrrolidine. We elaborated the resulting amines with several electrophiles (Figure 3A) and asked whether these compounds could label K-Ras mutant proteins. Although many of the compounds label K-Ras G12C at pH 7.5 with only minor nonspecific labeling of WT K-Ras, we did not observe labeling of K-Ras G12D CL in buffers ranging from pH 7.5 to 5.5 (Figure 3B). The aziridines did not efficiently label K-Ras G12C despite having reactivities toward benzoate and *N*-Boc-aspartate similar to those of **3** and **4**.

We next used DSF to compare all of the complexes of K-Ras G12C CL fully labeled with one of the compounds. Overall, complexes of compounds with longer linkers have higher melting temperatures (Figure 3C). It is likely that compounds with shorter effective linkers cause the loss of hydrogen bonding contacts after the reaction has occurred. For compounds with the same electrophile, we wondered whether compounds with higher melting temperatures would also have faster labeling rates. In contrast, compound **1** ($T_M = 77.7$ °C) labels Ras much more quickly than **11** does ($T_M = 78.7$ °C), despite having a roughly equivalent melting temperature (Figure 3D). Similarly, **6** ($T_M = 65.4$ °C) labels Ras more quickly than **13** does ($T_M = 65.1$ °C) (Figure 3E). More strikingly, **2** ($T_M = 68.7$ °C) stabilizes Ras less strongly than **12** does ($T_M = 73.4$ °C), but labels much more quickly (Figure S6). Disagreement between the melting temperature and labeling rate emphasizes a limitation of DSF as a tool for understanding the contribution of reversible binding to the formation of a covalent complex. The labeling rates of these compounds are also influenced by the spatial relationship between the electrophile and Cys12, the presence of a carbonyl–Lys16 hydrogen bond, and the presence of stereo-isomers that do not support covalent bond formation.

The ability of a covalent inhibitor to reversibly bind its target protein increases the effective molarity of the electrophile and promotes covalent bond formation.³² We wondered whether modest reversible binding might contribute to the low reactivity of these compounds toward Asp12. To improve our understanding of the reversible affinity of the quinazoline scaffold, we synthesized two non-electrophilic analogues, **21** and **22**. In DSF, addition of **21** and **22** (100 μ M) did not change the melting profile of K-Ras G12C CL (8 μ M) (Figure 4A). Similarly, addition of excess **21** or **22** (100 μ M) to a labeling reaction mixture did not appreciably weaken the ability of compound **6** (10 μ M) to label K-Ras G12C CL (4 μ M) (Figure 4B). Together, these results suggest that the reversible affinity of the quinazoline scaffold is weaker than 8 μ M. It is possible that substantially stronger reversible binding would allow covalent bond formation with a noncatalytic aspartate residue.

CONCLUSIONS

With the goal of expanding the types of electrophiles that are useful for targeting oncogenic K-Ras mutant proteins, we screened several electrophilic compounds for their ability to react with carboxylates and characterized the ability of aziridine and stabilized diazo groups to nonspecifically label Ras. We also characterized the ability of these electrophiles to covalently label K-Ras G12C, suggesting their potential utility in probes for cysteines that do not react with acrylamides. The complexes of these compounds with K-Ras G12C were further characterized by X-ray crystallography, hydrogen/deuterium exchange mass spectrometry, structural modeling, and DSF. The resulting data reveal that relatively minor changes in the electrophilic warhead can result in dramatic changes in the ligand binding mode and labeling rate, highlighting the need to optimize the spatial relationship between an electrophile and its amino acid nucleophile. We hope that these findings can broaden the array of electrophiles and nucleophiles of use in the covalent modulation of proteins.

Acknowledgments

We thank the staff at beamline 8.2.2 at the Advanced Light Source, which is a U.S. Department of Energy Office of Science User Facility under Contract DE-AC02-05CH11231.

Funding

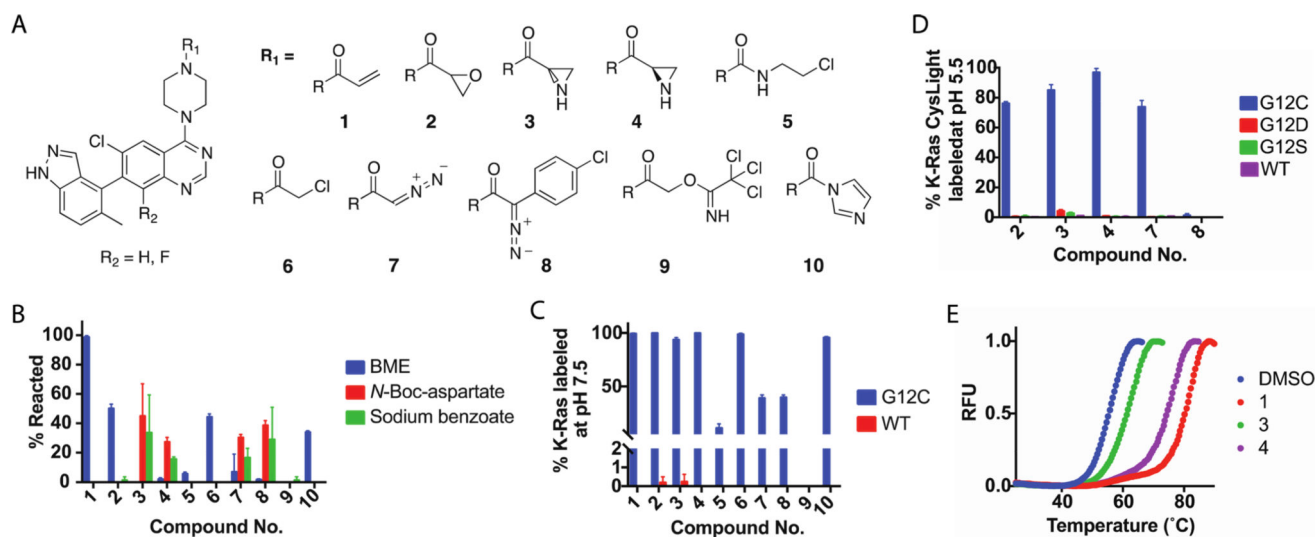
This work was supported by the Howard Hughes Medical Institute (K.M.S.), National Institutes of Health Grant R01 5R01CA190408 (K.M.S.), and a discovery research grant from the Natural Sciences and Engineering Research Council of Canada (NSERC-2014-05218) to J.E.B. This research was also supported by a Stand Up To Cancer-American Cancer Society Lung Cancer Dream Team Translational Research Grant (SU2C-AACR-DT17-15) (to K.M.S.). Stand Up to Cancer is a program of the Entertainment Industry Foundation. Research grants are administered by the American Association for Cancer Research, the scientific partner of SU2C. L.M.M. is a fellow of the American Cancer Society (PF-15-104-01-CDD) and acknowledges a 2015 Pancreatic Cancer Action Network - NCI, Frederick National Laboratory for Cancer Research KRAS Fellowship (15-25-40-McGregor). The project has also been funded in part by NCI Contract HHSN26120080001E.

References

1. Ostrem JML, Shokat KM. Direct small-molecule inhibitors of KRAS: from structural insights to mechanism-based design. *Nat. Rev. Drug Discovery*. 2016; 15:771–785. [PubMed: 27469033]
2. Prior IA, Lewis PD, Mattos C. A comprehensive survey of ras mutations in cancer. *Cancer Res*. 2012; 72:2457–2467. [PubMed: 22589270]
3. Burns MC, Sun Q, Daniels RN, Camper D, Kennedy JP, Phan J, Olejniczak ET, Lee T, Waterson AG, Rossanese OW, Fesik SW. Approach for targeting Ras with small molecules that activate SOS-mediated nucleotide exchange. *Proc. Natl. Acad. Sci. U. S. A.* 2014; 111:3401–3406. [PubMed: 24550516]
4. Sun Q, Burke JP, Phan J, Burns MC, Olejniczak ET, Waterson AG, Lee T, Rossanese OW, Fesik SW. Discovery of small molecules that bind to K-Ras and inhibit SOS-mediated activation. *Angew. Chem., Int. Ed.* 2012; 51:6140–6143.
5. Maurer T, Garrenton LS, Oh A, Pitts K, Anderson DJ, Skelton NJ, Fauber BP, Pan B, Malek S, Stokoe D, Ludlam MJC, Bowman KK, Wu J, Giannetti AM, Starovasnik MA, Mellman I, Jackson PK, Rudolph J, Wang W, Fang G. Small-molecule ligands bind to a distinct pocket in Ras and inhibit SOS-mediated nucleotide exchange activity. *Proc. Natl. Acad. Sci. U. S. A.* 2012; 109:5299–5304. [PubMed: 22431598]
6. Welsch ME, Kaplan A, Chambers JM, Stokes ME, Bos PH, Zask A, Zhang Y, Sanchez-Martin M, Badgley MA, Huang CS, Tran TH, Akkiraju H, Brown LM, Nandakumar R, Cremers S, Yang WS, Tong L, Olive KP, Ferrando A, Stockwell BR. Multivalent small-molecule pan-Ras inhibitors. *Cell*. 2017; 168:878–889.e29. [PubMed: 28235199]

7. Patgiri A, Yadav KK, Arora PS, Bar-Sagi D. An orthosteric inhibitor of the Ras-Sos interaction. *Nat. Chem. Biol.* 2011; 7:585–587. [PubMed: 21765406]
8. Ostrem JM, Peters U, Sos ML, Wells JA, Shokat KM. K-Ras(G12C) inhibitors allosterically control GTP affinity and effector interactions. *Nature.* 2013; 503:548–551. [PubMed: 24256730]
9. Lim SM, Westover KD, Ficarro SB, Harrison RA, Choi HG, Pacold ME, Carrasco M, Hunter J, Kim ND, Xie T, Sim T, Jänne PA, Meyerson M, Marto JA, Engen JR, Gray NS. Therapeutic targeting of oncogenic K-Ras by a covalent catalytic site inhibitor. *Angew. Chem., Int. Ed.* 2014; 53:199–204.
10. Mah R, Thomas JR, Shafer CM. Drug discovery considerations in the development of covalent inhibitors. *Bioorg. Med. Chem. Lett.* 2014; 24:33–39. [PubMed: 24314671]
11. Bandyopadhyay A, Gao J. Targeting biomolecules with reversible covalent chemistry. *Curr. Opin. Chem. Biol.* 2016; 34:110–116. [PubMed: 27599186]
12. Baillie TA. Targeted covalent inhibitors for drug design. *Angew. Chem., Int. Ed.* 2016; 55:13408–13421.
13. Backus KM, Correia BE, Lum KM, Forli S, Horning BD, González-Páez GE, Chatterjee S, Lanning BR, Teijaro JR, Olson AJ, Wolan DW, Cravatt BF. Proteome-wide covalent ligand discovery in native biological systems. *Nature.* 2016; 534:570–574. [PubMed: 27309814]
14. Visscher M, Arkin MR, Dansen TB. Covalent targeting of acquired cysteines in cancer. *Curr. Opin. Chem. Biol.* 2016; 30:61–67. [PubMed: 26629855]
15. Lin S, Yang X, Jia S, Weeks AM, Hornsby M, Lee PS, Nichiporuk RV, Iavarone AT, Wells JA, Toste FD, Chang CJ. Redox-based reagents for chemoselective methionine bioconjugation. *Science.* 2017; 355:597–602. [PubMed: 28183972]
16. Narayanan A, Jones LH. Sulfonyl fluorides as privileged warheads in chemical biology. *Chem. Sci.* 2015; 6:2650–2659. [PubMed: 28706662]
17. Shannon DA, Weerapana E. Covalent protein modification: the current landscape of residue-specific electrophiles. *Curr. Opin. Chem. Biol.* 2015; 24:18–26. [PubMed: 25461720]
18. Martín-Gago P, Fansa EK, Winzker M, Murarka S, Janning P, Schultz-Fademrecht C, Baumann M, Wittinghofer A, Waldmann H. Covalent protein labeling at glutamic acids. *Cell Chem. Biol.* 2017; 24:589–597. [PubMed: 28434875]
19. Weerapana E, Simon GM, Cravatt BF. Disparate proteome reactivity profiles of carbon electrophiles. *Nat. Chem. Biol.* 2008; 4:405–407. [PubMed: 18488014]
20. Benedetti F, Berti F, Campaner P, Fanfoni L, Demitri N, Olajuyigbe FM, De March M, Geremia S. Impact of stereochemistry on ligand binding: x-ray crystallographic analysis of an epoxide-based HIV protease inhibitor. *ACS Med. Chem. Lett.* 2014; 5:968–972. [PubMed: 25221650]
21. Los GV, Encell LP, McDougall MG, Hartzell DD, Karassina N, Zimprich C, Wood MG, Learish R, Ohana RF, Urh M, Simpson D, Mendez J, Zimmerman K, Otto P, Vidugiris G, Zhu J, Darzins A, Klaubert DH, Bulleit RF, Wood KV. HaloTag: a novel protein labeling technology for cell imaging and protein analysis. *ACS Chem. Biol.* 2008; 3:373–382. [PubMed: 18533659]
22. Trzeciakiewicz A, Fortin S, Moreau E, C-Gaudreault R, Lacroix J, Chambon C, Communal Y, Chezal J-M, Miot-Noirault E, Bouchon B, Degoul F. Intramolecular cyclization of N-phenyl N'(2-chloroethyl)ureas leads to active N-phenyl-4,5-dihydrooxazol-2-amines alkylating β -tubulin Glu198 and prohibitin Asp40. *Biochem. Pharmacol.* 2011; 81:1116–1123. [PubMed: 21371445]
23. McGrath NA, Andersen KA, Davis AKF, Lomax JE, Raines RT. Diazo compounds for the bioreversible esterification of proteins. *Chem. Sci.* 2015; 6:752–755. [PubMed: 25544883]
24. Mix KA, Raines RT. Optimized diazo scaffold for protein esterification. *Org. Lett.* 2015; 17:2358–2361. [PubMed: 25938936]
25. Shah JP, Russo CM, Howard KT, Chisholm JD. Spontaneous formation of PMB esters using 4-methoxybenzyl-2,2,2-trichloroacetimidate. *Tetrahedron Lett.* 2014; 55:1740–1742.
26. Fujishima S-H, Yasui R, Miki T, Ojida A, Hamachi I. Ligand-directed acyl imidazole chemistry for labeling of membrane-bound proteins on live cells. *J. Am. Chem. Soc.* 2012; 134:3961–3964. [PubMed: 22352855]
27. Patricelli MP, Janes MR, Li L-S, Hansen R, Peters U, Kessler LV, Chen Y, Kucharski JM, Feng J, Ely T, Chen JH, Firdaus SJ, Babbar A, Ren P, Liu Y. Selective inhibition of oncogenic KRAS output with small molecules targeting the inactive state. *Cancer Discovery.* 2016; 6:316–329. [PubMed: 26739882]

28. Li, L., Feng, J., Ren, P., Liu, Y. Inhibitors of KRas G12C. U.S. Patent Application. 14/511,425. 2015.
29. Niesen FH, Berglund H, Vedadi M. The use of differential scanning fluorimetry to detect ligand interactions that promote protein stability. *Nat. Protoc.* 2007; 2:2212–2221. [PubMed: 17853878]
30. Gallagher ES, Hudgens JW. Mapping protein-ligand interactions with proteolytic fragmentation, hydrogen/deuterium exchange-mass spectrometry. *Methods Enzymol.* 2016; 566:357–404. [PubMed: 26791987]
31. Harrison RA, Lu J, Carrasco M, Hunter J, Manandhar A, Gondi S, Westover KD, Engen JR. Structural dynamics in Ras and related proteins upon nucleotide switching. *J. Mol. Biol.* 2016; 428:4723–4735. [PubMed: 27751724]
32. Singh J, Petter RC, Baillie TA, Whitty A. The resurgence of covalent drugs. *Nat. Rev. Drug Discovery.* 2011; 10:307–317. [PubMed: 21455239]

**Figure 1.**

(A) Optimized ligand of the Ras switch II pocket elaborated with a set of electrophiles. (B) Aziridine and stabilized diazo groups preferentially react with carboxylates at pH 6. (C) Many of the electrophiles covalently label K-Ras G12C. (D) Compound **3** modestly labels G12D and G12S at pH 5.5. (E) DSF suggests that **3** and **4** may bind Ras differently.

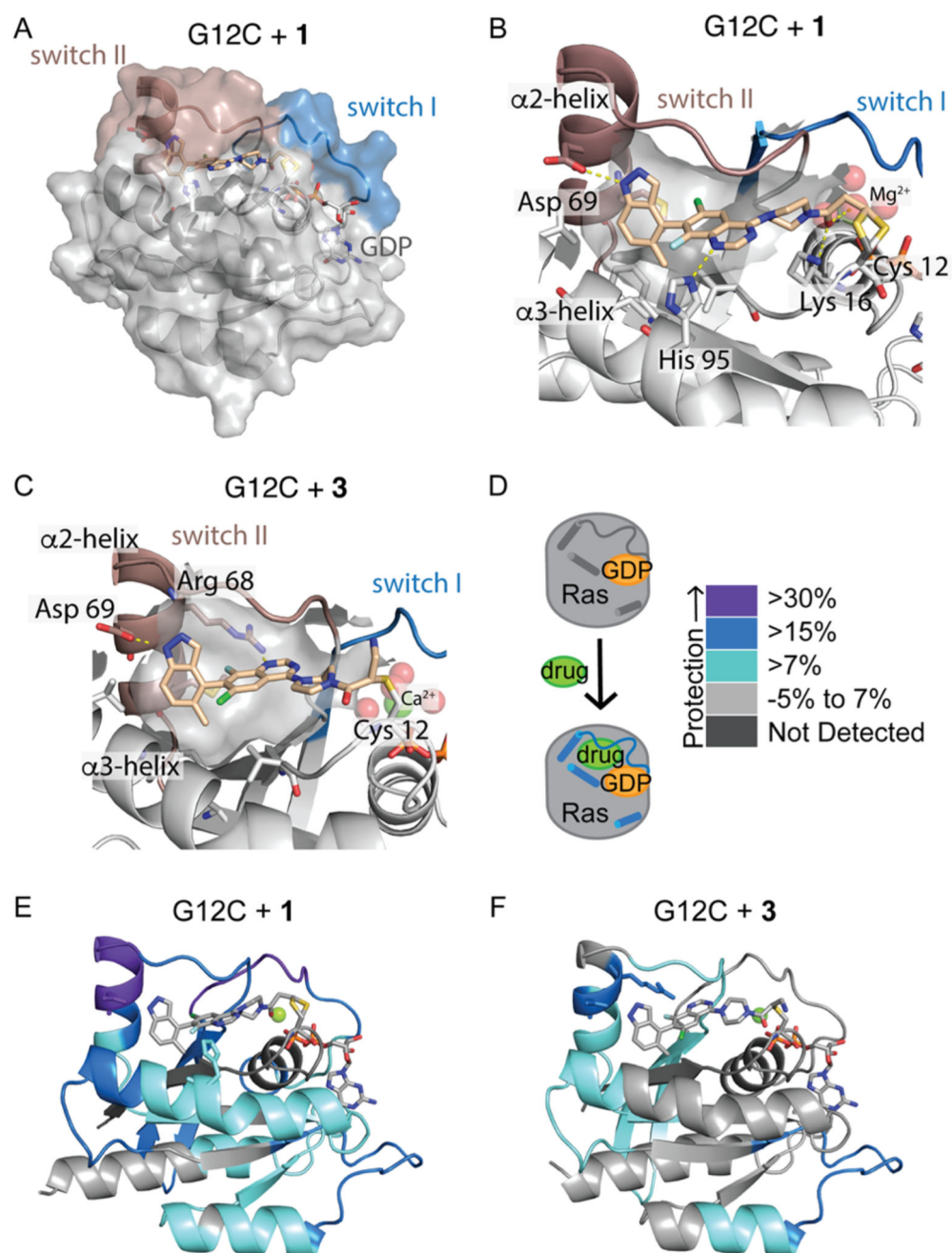
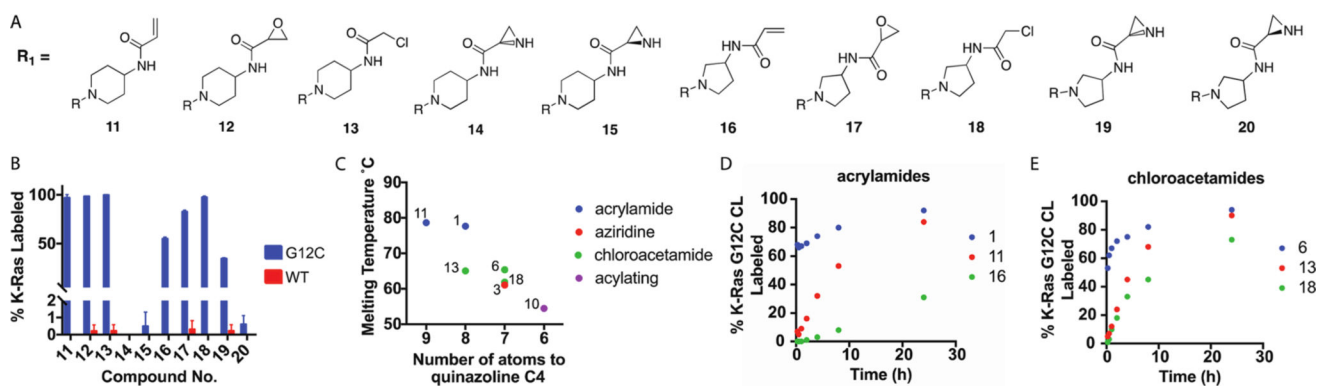


Figure 2. (A and B) Compound **1** is surrounded by switch II and makes many contacts with the switch II pocket. (C) Compound **3** binds via the opposite atropisomer as **1**. (D) HDX measures the effect of **1** and **3** on protein dynamics. (E and F) Peptides showing significant differences in HDX at any time point (>0.6 Da and >6%) are mapped onto the corresponding structure according to the legend in panel D.

**Figure 3.**

(A) Piperazine linker that was replaced with an exocyclic amine and elaborated with several electrophiles. (B) Compounds **11–13** and **16–19** label K-Ras G12C. (C) DSF shows a relationship between stabilization and the position of the electrophilic atom. Compounds with an ambiguous site of labeling are not shown. (D) Despite equivalent stabilization, **1** labels K-Ras G12C more quickly than **11** does. (E) For the chloroacetamides, **6** labels much more rapidly than the equivalently stabilizing **13** does.

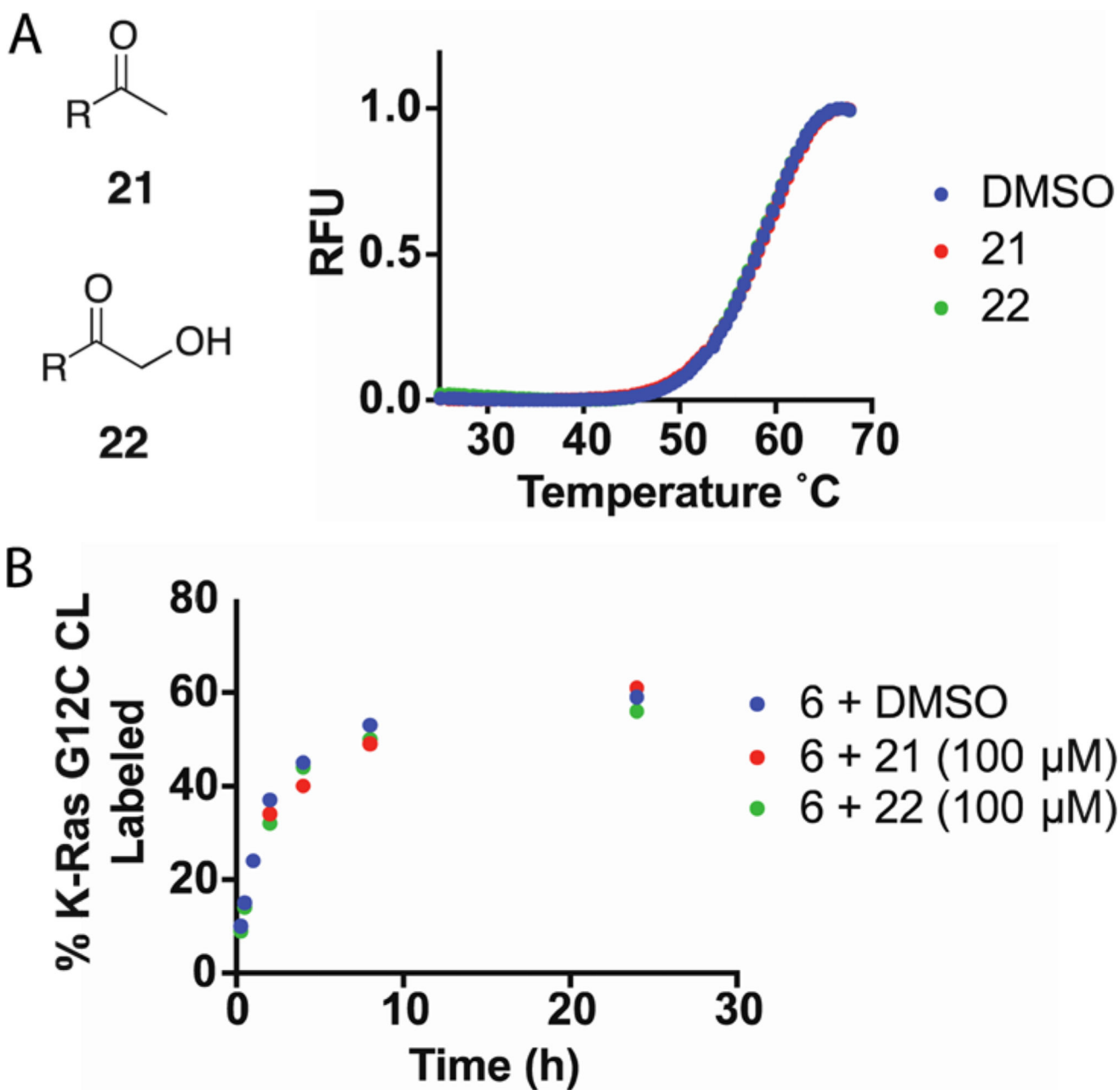


Figure 4.

(A) Noncovalent compounds **21** and **22** (100 μ M) did not alter the DSF profile of K-Ras G12C CL (8 μ M). (B) Competition with excess **21** or **22** (100 μ M) did not decrease the rate of labeling of **6** (10 μ M).